



University of Groningen

## Uncoupling in Secondary Transport Proteins. A Mechanistic Explanation for Mutants of lac Permease with an Uncoupled Phenotype

Lolkema, J.S.; Poolman, B.

*Published in:*  
The Journal of Biological Chemistry

*DOI:*  
[10.1074/jbc.270.21.12670](https://doi.org/10.1074/jbc.270.21.12670)

**IMPORTANT NOTE:** You are advised to consult the publisher's version (publisher's PDF) if you wish to cite from it. Please check the document version below.

*Document Version*  
Publisher's PDF, also known as Version of record

*Publication date:*  
1995

[Link to publication in University of Groningen/UMCG research database](#)

### *Citation for published version (APA):*

Lolkema, J. S., & Poolman, B. (1995). Uncoupling in Secondary Transport Proteins. A Mechanistic Explanation for Mutants of lac Permease with an Uncoupled Phenotype. *The Journal of Biological Chemistry*, 270(21), 12670-12676. <https://doi.org/10.1074/jbc.270.21.12670>

### **Copyright**

Other than for strictly personal use, it is not permitted to download or to forward/distribute the text or part of it without the consent of the author(s) and/or copyright holder(s), unless the work is under an open content license (like Creative Commons).

### **Take-down policy**

If you believe that this document breaches copyright please contact us providing details, and we will remove access to the work immediately and investigate your claim.

*Downloaded from the University of Groningen/UMCG research database (Pure): <http://www.rug.nl/research/portal>. For technical reasons the number of authors shown on this cover page is limited to 10 maximum.*

# Uncoupling in Secondary Transport Proteins

A MECHANISTIC EXPLANATION FOR MUTANTS OF *lac* PERMEASE WITH AN UNCOUPLED PHENOTYPE\*

(Received for publication, June 14, 1994, and in revised form, October 19, 1994)

Juke S. Lolkema† and Bert Poolman‡

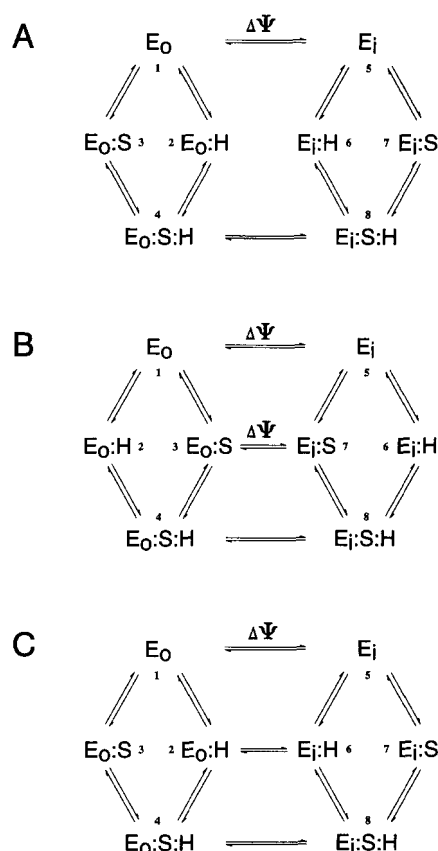
From the Department of Microbiology, Groningen Biomolecular Sciences and Biotechnology Institute, University of Groningen, Kerklaan 30 9751 NN HAREN, The Netherlands

The kinetic behavior of a  $H^+$ -substrate symporter has been studied in which in addition to the unloaded ( $E$ ) and fully loaded states ( $E \cdot S \cdot H$ ) of the carrier also one of the binary complexes ( $E \cdot S$  or  $E \cdot H$ ) may reorient its binding sites. This results in two types of uncoupled mutants, the ES leak and the EH leak type. The effects of pH and substrate concentration (pS) on the coupling of transport have been analyzed. In the enzyme with the ES leak, the proton:substrate stoichiometry ( $v(H^+)/v(S)$ ) and the substrate accumulation levels decrease sigmoidally from fully coupled at low pH to completely uncoupled at high pH. Importantly, the coupling inferred from initial rate measurements is higher than from steady state accumulation levels. In the enzyme with the EH leak, the coupling inferred from the accumulation levels increases from no coupling at low pH to full coupling at high pH and saturating substrate concentration. The  $v(H^+)/v(S)$  increases sigmoidally with pH from  $<1$  to  $>1$  and is highly dependent on pS. At each pH value a substrate concentration can be found that results in apparent complete coupling between the two fluxes.

The ES leak and the EH leak mutants provide a mechanism for substrate-induced and substrate-inhibited proton leakage, respectively. Furthermore, substrate efflux down a concentration gradient is inhibited by a membrane potential (inside negative) under uncoupled conditions in the case of an ES leak but not in the case of an EH leak.

The properties of the mutants mimic those of various transport mutants that have been described, in particular mutants of the lactose transport protein of *Escherichia coli*. The analysis offers general means for targeted experimentation, which allows discrimination between various types of transport mutants.

It is generally believed that catalysis by a proton symporter proceeds via the formation of a ternary complex among substrate, proton, and carrier as depicted in Scheme 1A. The binding sites for proton and substrate are oriented simultaneously toward either the outside or the inside of the cell. The “unloaded” states of the carrier,  $E_o$  and  $E_i$ , and the fully loaded states,  $E_o \cdot S \cdot H$  and  $E_i \cdot S \cdot H$ , are mobile forms of the carrier, *i.e.* they can reorient the binding sites spontaneously. In contrast, the binary complexes between carrier and either substrate are immobile. The membrane potential is believed to exert its kinetic



SCHEME I. Kinetic schemes for the wild-type proton-symporter (A), the ES leak type of mutant (B), and the EH leak type of mutant (C). Subscripts o and i denote the external and internal orientation of the binding sites on the enzyme, respectively. The steps that are affected by the membrane potential are indicated by  $\Delta\psi$ .

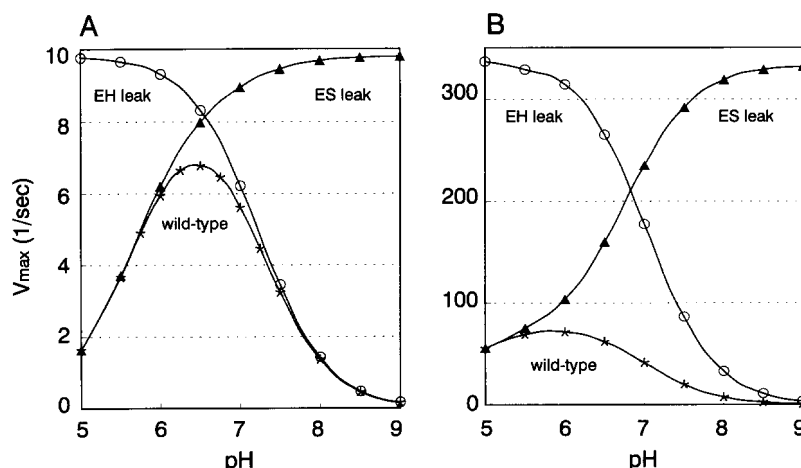
effect on one of the mobile forms, in the case of LacY, the lactose transport protein of *E. coli*, the unloaded carrier (Garcia *et al.*, 1983). The coupling of substrate and proton flux is a direct consequence of the mobile and immobile states of the carrier (for a recent discussion see Krupka (1993)). Reorientation of the binding sites and, therefore, transport takes place only after both proton and substrate have bound to their respective binding sites. Binding of one of the two substrates to the unloaded carrier changes the carrier from a mobile to an immobile state. The carrier becomes “locked” in a state with the binding sites oriented toward the side of the membrane from which the binding took place. Both substrates can lock the carrier independently of each other in the immobile state. Therefore, we postulate that two types of mutants with an uncoupled phenotype can be found: the “ES leak” type and the “EH leak” type (Scheme I, B and C, respectively). Binding of the substrate to

\* The costs of publication of this article were defrayed in part by the payment of page charges. This article must therefore be hereby marked “advertisement” in accordance with 18 U.S.C. Section 1734 solely to indicate this fact.

† To whom correspondence should be addressed. Tel.: 31-50-632155; Fax: 31-50-632154; E-mail: LOKEMA@BIOL.RUG.NL.

‡ Recipient of a grant from the Human Frontier Science Program Organization (HFSP).

FIG. 1. The maximal rate of substrate uptake of the wild-type enzyme (\*), the ES leak mutant ( $\blacktriangle$ ), and the EH leak mutant ( $\circ$ ) at different pH values. A, rapid binding equilibria. B, non-rapid binding equilibria. The rate constants used in the simulations are described under "Materials and Methods." The initial rates were calculated in the presence of a pH gradient, inside alkaline, of 1 unit (pmf = -60 mV). The indicated pH value is that of the external pH.



the unloaded carrier in the ES leak type does not result in locking of the carrier, whereas binding of the proton does. In the EH leak type this is just the other way around.

In the present paper we analyze the behavior of the ES leak and the EH leak types of uncoupled mutants in steady state kinetic measurements. It is demonstrated that the degree of coupling may be very different when inferred from initial rate measurements or steady state accumulation levels. The analysis suggests ways to discriminate relatively easily between mutants with an ES or EH leak. This pinpoints the mutated residues to the interactions between carrier and substrate or carrier and proton. Some properties of the hypothetical enzymes are strikingly similar to those of various LacY mutants listed in Table I.

#### MATERIALS AND METHODS

The kinetic behavior of the wild-type enzyme and the uncoupled mutants was analyzed by numerical solution of the steady state equations using the computer program CACES (Lolkema, 1993). The basic set of rate constants pertinent to Scheme 1A used in the simulations was as follows. The affinity constant for the substrate was 1 mM with rate constants of  $1000 \text{ mM}^{-1} \text{ s}^{-1}$  and  $1000 \text{ s}^{-1}$ , respectively. The pK of the proton binding site was 7 with  $1000 \mu\text{M}^{-1} \text{ s}^{-1}$  and  $100 \text{ s}^{-1}$  for the rate constants. The rate constants pertinent to the translocation of the unloaded carrier and the ternary complex were  $20 \text{ s}^{-1}$  in both directions. This set corresponds to a symmetrical carrier with rapid binding equilibria relative to the translocation equilibria. In a second set the binding equilibria were made slow relative to the translocation equilibria by increasing the rate constants of the latter to  $2000 \text{ s}^{-1}$ . This set will be referred to as non-rapid binding equilibria. The rate constants for the translocation of the binary complexes were set to zero in the kinetic scheme representing the wild-type carrier. Unless otherwise stated, in the ES leak type of mutant (Scheme 1B) the rate constants for the translocation of the enzyme-substrate complex E·S were made identical to the translocation rate constants of the wild-type translocations. The same adjustment was made to the rate constants for the translocation of the protonated carrier E·H in the EH leak type of mutant (Scheme 1C).

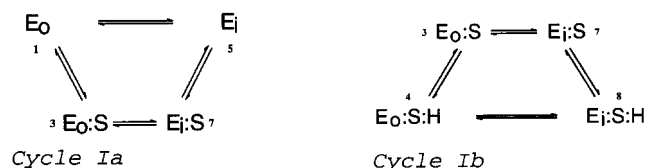
A membrane potential  $\Delta\psi$  was included in the simulations by affecting the forward and backward rate constants ( $k_{oi}$  and  $k_{io}$ , respectively) of selected translocation equilibria as follows:  $k_{oi} = k_{oi}^0 \exp(0.5\Delta\psi/RT)$  and  $k_{io} = k_{io}^0 \exp(-0.5\Delta\psi/RT)$ .

#### RESULTS

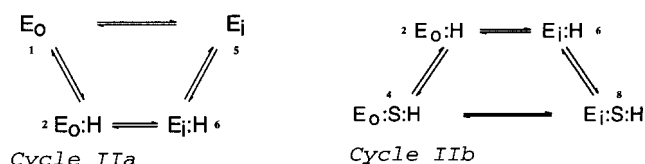
**Kinetics of the Wild-type Enzyme and Uncoupled Mutants—**The maximal rate of proton motive force (pmf)<sup>1</sup>-driven substrate uptake catalyzed by the fully coupled enzyme follows a bell-shaped curve when simulated at different pH values, irrespective of whether the binding steps are fast or slow relative to the translocations (Fig. 1, A and B, asterisk). The pH dependence is the result of two counteracting steps in the catalytic cycle, i.e. the

protonation and deprotonation of the carrier at the external and internal face of the membrane, respectively (see Scheme 1A). Since both steps are obligatory for turnover, the highest rates are observed at intermediate pH values. At lower pH values the enzyme piles up in state  $E_i\cdot H$  (state 6), at higher pH the enzyme piles up in state  $E_o\cdot S$  (3). The highest maximal rate is observed at pH 7 (the pK of the proton binding sites) in the case of facilitated influx or efflux (data not shown) and is shifted toward more acidic values in the presence of a pmf (Fig. 1).

In the case of the ES leak (Scheme 1B), the maximal rate of uptake increases with pH and reaches a plateau at alkaline pH values (Fig. 1, A and B,  $\blacktriangle$ ). The ES leak opens up two alternative routes for turnover of the carrier (cycles 1a and 1b).



Cycle 1a represents facilitated diffusion of the substrate catalyzed by the unprotonated carrier. It prevails at high pH values and compensates for the decreased rate of uptake at higher pH values observed with the wild-type enzyme. At low pH values, the major pathway proceeds via the translocation of the ternary complex. Cycle 1b depicts a transport mode for the proton catalyzed by the enzyme-substrate complex E·S. Under conditions of accumulation of the substrate inside the cell, i.e. when state  $E_i\cdot S$  becomes populated, the cycle provides a slip for the proton.



Introduction of the EH leak results in two similar cycles. Cycle 1Ia provides a pathway for the proton, resulting in a proton leak in the absence of substrate. Cycle 1Ib represents a facilitated diffusion cycle for the substrate catalyzed by the protonated carrier. It compensates for the decrease in the rate at low pH values observed with the wild-type enzyme (Fig. 1, A and B,  $\circ$ ). At low pH values cycle 1Ib is the major pathway,

<sup>1</sup> The abbreviation used is: pmf, proton motive force.

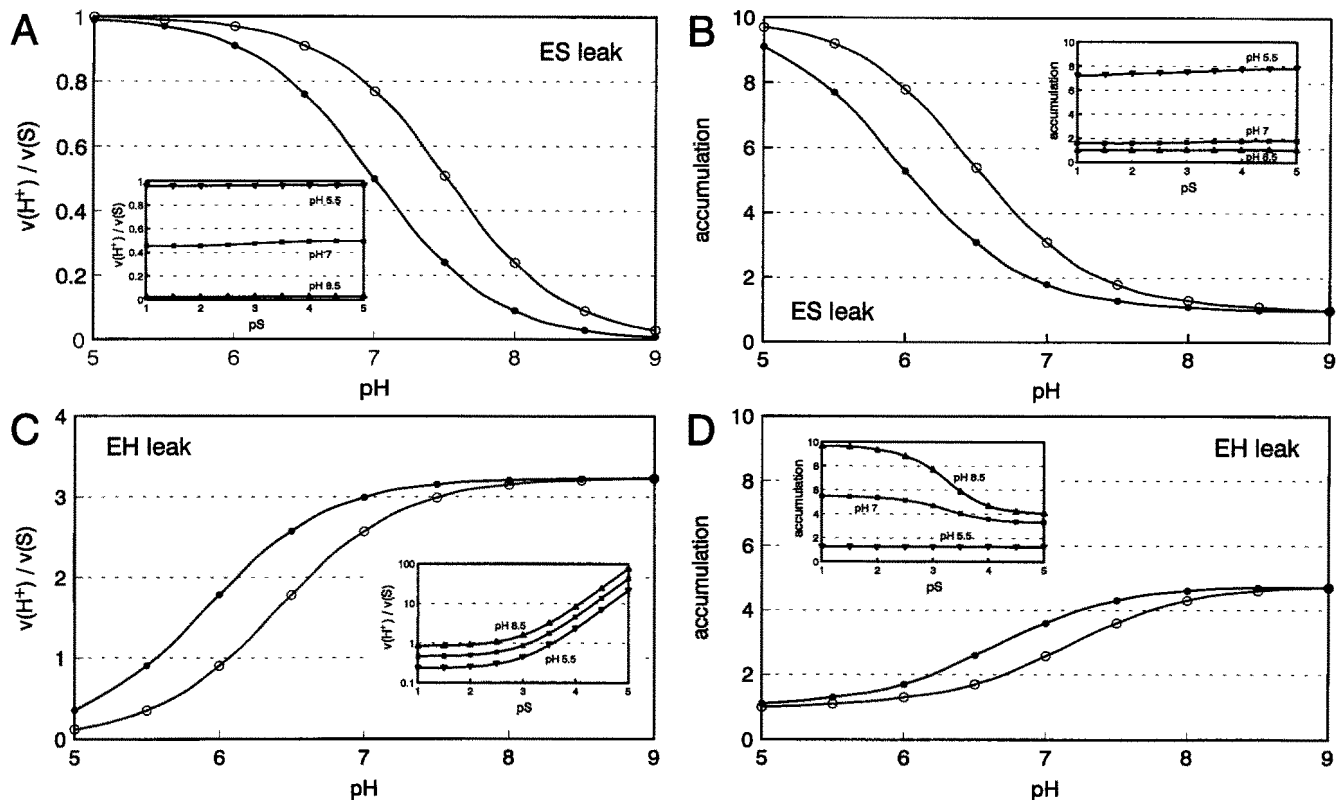


FIG. 2. The coupling stoichiometry as a function of pH for the ES leak (A, B) and EH leak (C, D) mutants. Panels A and C show the ratio of the initial rates of uptake of proton and substrate. Panels B and D show the accumulation of the substrate in the cell under conditions of zero flux for the substrate (kinetic steady state). The rates and accumulation levels were calculated in the presence of a pH gradient (●) and a membrane potential (○) of  $-60$  mV. In the case of a fully coupled enzyme this would result in an accumulation ratio of 10. The insets show the dependences on the substrate concentration in the presence of a pH gradient of  $-60$  mV at pH 5.5 (▼), pH 7 (■), and pH 8.5 (▲). The intermediate pH in the inset of Fig. 2C is pH 6 (■). The y axis in the inset of Fig. 2C is logarithmic.

whereas at high pH the major pathway is via states  $E_i$  and  $E_o$ .

The affinity constants for the substrate of the transport activities shown in Fig. 1 show a sigmoidal increase with pH. Introduction of the leaks does not result in dramatic changes in the  $K_m$  values. At the pH optimum the affinity constants range from 0.6 to 1.1 mM and from 0.5 to 1.7 mM in the case of rapid binding equilibria and non-rapid binding equilibria, respectively.

Both in the ES leak and the EH leak the carrier shifts from symport to uniport and *vice versa* as a function of pH. The different cycles introduced by the two leaks result in significant different kinetic behavior of the enzyme under various conditions (see below).

**Proton:Substrate Stoichiometries**—The coupling stoichiometry of secondary transporters is inferred either from the accumulation of the substrate inside the cells in the presence of a pmf of known magnitude or from the ratio of the initial rates of uptake of the substrate and the proton. Thermodynamic considerations of the catalyzed symport reaction require that at equilibrium the force on the substrate is counteracted by the force on the proton.

$$\Delta\mu_s = -n_{\text{grad}}\Delta\mu_{\text{H}^+} \quad (\text{Eq. 1})$$

The chemical potential gradient  $\Delta\mu_s$  corresponds to the accumulation ratio of substrate inside and outside the cell under zero flux conditions for the substrate. In a fully coupled enzyme, the stoichiometric coefficient  $n_{\text{grad}}$ , which balances both gradients, equals the stoichiometric coefficient of the catalyzed reaction  $n_{\text{kin}}$  that follows from initial rate measurements.

$$v(\text{H}^+) = n_{\text{kin}}v(\text{S}) \quad (\text{Eq. 2})$$

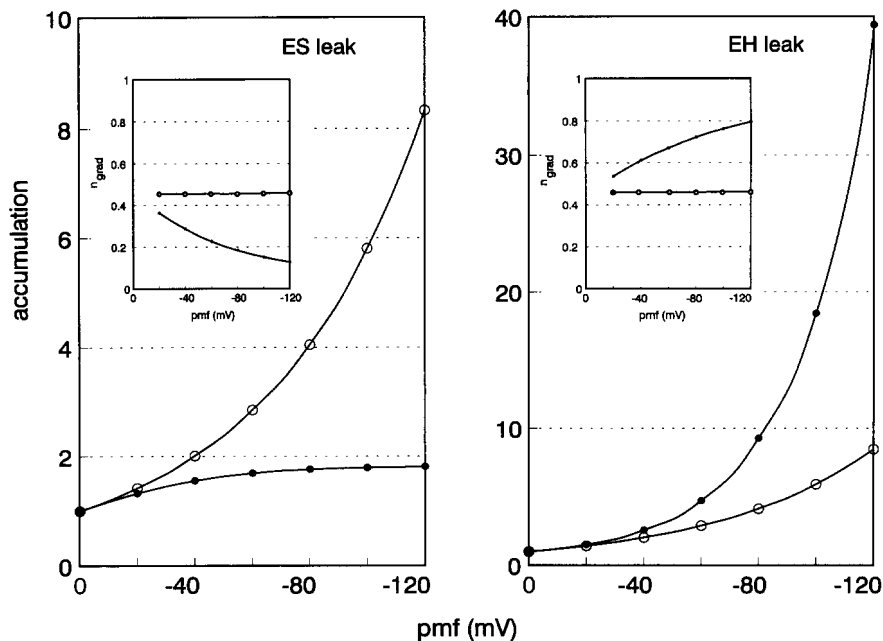
In the fully coupled carrier depicted in Scheme 1A, the coupling

stoichiometry will be 1 irrespective of the method used for the measurement or the condition of the carrier. The coupling is determined by the kinetic scheme. In contrast, introduction of the uncoupling pathways (Scheme 1, B and C) results in stoichiometries that not only depend on the conditions but may also be significantly different when inferred from accumulation ratios or initial rate ratios.

In the case of a mutant with an ES leak, the ratio of the initial rates of uptake of proton and substrate decreases sigmoidally from 1 at low to 0 at high pH values both with  $\Delta\psi$  and  $\Delta\text{pH}$  as driving force (Fig. 2A). At low pH, the major pathway is the same as in the wild-type enzyme and, consequently, the two fluxes are fully coupled. Increasing the pH results in an increasing contribution of cycle Ia to the flux with a subsequent decrease in the rate of proton influx. The stoichiometries are largely independent of the substrate concentration when the binding equilibria are fast (Fig. 2A, inset). Increasing the rate constants for the translocations has no effect on the coupling at low substrate concentrations but results in reduced coupling at higher substrate concentrations (not shown). The accumulation levels under zero flux conditions for the substrate show a similar dependence on the pH. Accumulation is high at low pH values and negligible at high pH values (Fig. 2B). Also, the accumulation levels are independent of the substrate concentration in the case of rapid binding equilibria (Fig. 2B, inset) and are reduced in the case of non-rapid binding equilibria at high substrate concentrations. An important difference between the two experimental approaches is that at a given pH value the coupling inferred from accumulation ratios is significantly lower than from initial rate measurements.

The pH profile of the mutant with an EH leak is opposite to

FIG. 3. Accumulation efficiency in response to a membrane potential and a pH gradient. The accumulation under zero flux condition for the substrate was calculated in the presence of an external substrate concentration of 1 mM and at pH 7. The pmf consisted either of a membrane potential ( $\circ$ ) or a pH gradient ( $\bullet$ ). The inset shows the degree of coupling,  $n_{\text{grad}}$  (Equation 2).



that of the mutant with an ES leak. The ratio of the initial rates of proton uptake and substrate uptake increases with increasing pH (Fig. 2C). The ratio ranges from values below 1 at low pH to values above 1 at high pH, showing that the proton flux can be slower or faster than the substrate flux depending on the conditions. In contrast to what was observed with the ES leak, already with the rapid binding equilibria, the ratio of proton to substrate flux is strongly dependent on the substrate concentration (Fig. 2C, inset). With the non-rapid binding equilibria the curves in the inset of Fig. 2C shift to the right, resulting in a lower proton to substrate flux ratio at a fixed substrate concentration. Increasing concentrations of substrate decrease the degree of coupling from initial rates by pulling the enzyme in the ternary complex, thereby reducing the uncoupled proton flux via cycle IIA. The EH leak results in accumulation levels that also increase sigmoidally with pH (Fig. 2D). The substrate flux follows the uncoupled pathway via cycle IIB at low pH and the coupled pathway of the wild-type enzyme at high pH. The uncoupled pathway does not result in accumulation, independent of the substrate concentration used. Toward higher pH values the accumulation becomes more and more dependent on the substrate concentration, resulting in full coupling at high substrate concentrations (Fig. 2D, inset). In the case of non-rapid binding equilibria the concentration of substrate needed to achieve full coupling at high pH is higher (data not shown). The effect of the substrate concentration on the degree of coupling is opposite for initial rate measurements and accumulation.

In the case of an ES leak, both the stoichiometries from initial rates and accumulation are higher in the presence of a membrane potential than in the presence of a pH gradient of the same magnitude. This is just opposite for the EH leak. The effects of the membrane potential and pH gradient on the accumulation of substrate are analyzed in more detail in Fig. 3. The difference in accumulation in response to a membrane potential or a pH gradient increases with increasing magnitude of the forces. Analysis of the degree of coupling,  $n_{\text{grad}}$  (see Equation 1), indicates that in both types of mutants the coupling does not change with the membrane potential but decreases with the pH gradient in the ES leak and increases with the pH gradient in the EH leak (Fig. 3, insets). A change in the degree of coupling requires a change in the relative contributions of coupled and uncoupled pathways. With the ES leak, the

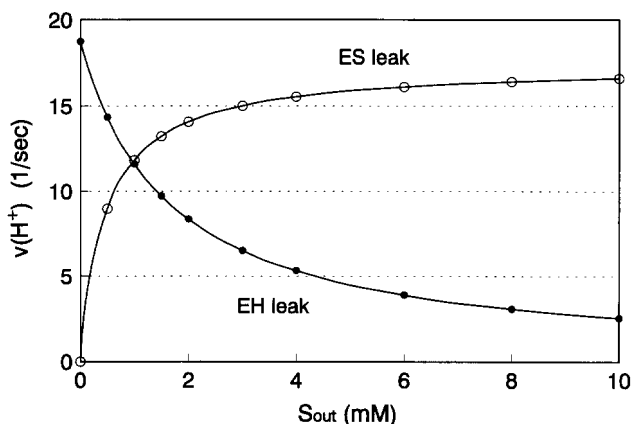


FIG. 4. Substrate-induced and -inhibited proton leaks. The net proton flux was calculated under condition of zero substrate flux, i.e. the substrate is equilibrated over the membrane, and in the presence of a pH gradient of  $-60$  mV.  $\circ$ , ES leak. The rate constants for the translocation of the ternary  $E\cdot S\cdot H$  and binary  $E\cdot S$  complex were set to  $200\text{ s}^{-1}$ . The association and dissociation rate constants for the binding equilibrium between the proton and the  $E\cdot S$  complex were set to  $5000\text{ }\mu\text{M}^{-1}\text{ s}^{-1}$  and  $500\text{ s}^{-1}$ . The external and internal pH values were 8 and 9, respectively. Under these conditions the substrate accumulation ranged from 1.49 at  $0.5\text{ mM}$  to 1.28 at  $10\text{ mM}$  of substrate.  $\bullet$ , EH leak. The rate constants for the translocation of the unloaded carrier and binary  $E\cdot H$  complex were set to  $200\text{ s}^{-1}$ . The external and internal pH were 6 and 7, respectively. The accumulation of the substrate ranged from 1.44 at  $0.5\text{ mM}$  to 1.73 at  $10\text{ mM}$  substrate.

relative contributions of the uncoupled pathway via cycle Ia and the coupled pathway are determined by the state of protonation of the carrier on the outside. Therefore, increasing the pH gradient by increasing the internal pH will not result in higher accumulation levels, i.e. the degree of coupling decreases. With the EH leak, the increase of the internal pH favors deprotonation of the carrier on the inside, which results in an increase of the coupled relative to the uncoupled pathway (cycle IIB), i.e. the degree of coupling increases.

**The Proton Leak under Zero Flux Conditions for the Substrate**—The wild-type proton symporter does not catalyze net proton transport after equilibration of the substrate inside the cell. A mutant with an ES leak cannot transport protons in the absence of substrate. However, the rate of proton influx under zero flux conditions for the substrate increases rapidly with

increasing external substrate concentrations (Fig. 4, ○). Apparently, the substrate induces a  $H^+$  leak corresponding to cycle Ib in the kinetic scheme for the mutant with the ES leak. The proton symporter with the EH leak confronts the cell with a continuous influx of protons via cycle IIa. Fig. 4 (●) shows the inhibition of the proton flux by equilibration of the cells with substrate. The presence of substrate at both sides of the membrane reduces the flux through cycle IIa by pulling the enzyme in the enzyme-substrate complex ( $E \cdot S \cdot H$ ).

**Kinetic Effect of the Membrane Potential under Uncoupled Conditions**—Thermodynamically, the pH gradient and the membrane potential are equivalent, i.e. a pH gradient and a membrane potential of the same magnitude result in the same level of accumulation of the substrate by the wild-type enzyme. Kinetically, the two gradients are not equivalent since they act on different steps in the kinetic scheme. While the pH gradient reflects different external and internal proton concentrations, the membrane potential affects the rate constants for the isomerization of the unloaded carrier (Scheme 1). A membrane potential of physiological polarity speeds up the transition from state  $E_i$  to  $E_o$  and inhibits the transition in the opposite direc-

tion. Therefore, the rate of efflux of substrate down a concentration gradient catalyzed by a wild-type symporter is inhibited by a membrane potential of normal polarity (inside negative).

The pH profiles of the efflux activities of the wild-type enzyme and the mutants with the ES leak and the EH leak are similar to the profiles shown in Fig. 1 for influx. Mutants with the ES leak are characterized by a high rate of efflux at high pH, which is catalyzed by the unprotonated carrier as described by cycle Ia. Both translocation steps in cycle Ia are affected by the membrane potential. The membrane potential tends to speed up efflux through its effect on the transition between  $E \cdot S_i$  and  $E \cdot S_o$  but inhibits efflux through its effect on the transition between  $E_o$  and  $E_i$ . The latter step becomes rate-limiting as the membrane potential increases. The net effect is an inhibition of the rate of efflux by the membrane potential under conditions where the carrier catalyzes essentially uniport of the substrate (Fig. 5, ○). Mutants with an EH leak show high rates of efflux at low pH values. Cycle IIb is responsible for the efflux. None of the steps in this cycle are affected by the membrane potential, and, consequently, the rate of efflux under these conditions is not significantly affected by the membrane potential (Fig. 5, ●).

#### DISCUSSION

Functional analysis of mutant secondary transporter enzymes may yield important information about residues involved in substrate and proton binding, translocation, coupling, etc. Such studies will also improve our knowledge about the kinetic mechanism of the wild-type enzyme. However, in spite of major efforts by a number of laboratories it has proven to be difficult to associate (mutated) residues with specific steps in the kinetic mechanism. In part, this is caused by the complicated relation between the kinetic behavior and the role of individual residues. In this study we analyze the kinetic behavior of two types of uncoupled mutants, those with mobile enzyme-substrate (ES leak) and enzyme-proton (EH leak) complexes. The two mechanisms of uncoupling are directly linked to the binding of substrate and proton (see Introduction), and, therefore, mutated residues that result in either type of uncoupling are involved in the events that follow upon the binding of substrate or proton to the carrier. The ability to discriminate between residues involved in substrate or proton binding adds a lot of detail to the role of the individual residues. It should be stressed that the analysis is general to symporters, irrespective

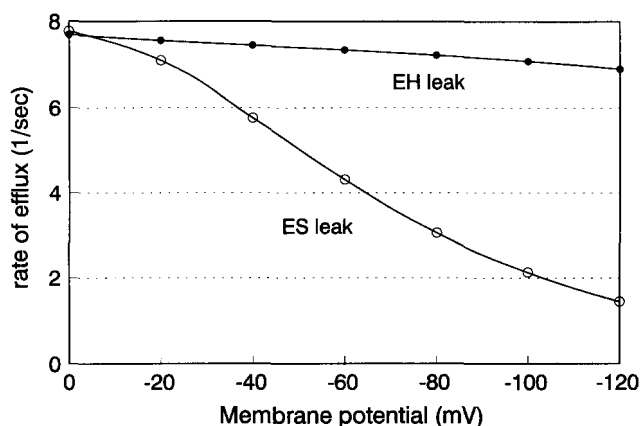


FIG. 5. Inhibition of efflux by the membrane potential under uncoupled conditions. The rate of efflux was calculated at pH 8 for the ES leak (○) and at pH 6 for the EH leak (●). The internal substrate concentration was 5 mM. At the same pH values, the substrate accumulation ratios of substrate at a membrane potential of  $-120$  mV and 1 mM of external substrate are 1.85 and 1.9 in the case of the ES leak and EH leak, respectively. The wild-type enzyme would accumulate the substrate by a factor of 100 at a membrane potential of  $-120$  mV.

TABLE I  
Properties of LacY mutants defective in energy coupling to transport

+, 100% activity; +/-, 10 < activity < 100%; -, no activity; LAC, lactose; TMG, thiomethylgalactoside; ND, not determined; ↓, down; ↑, up.					
Protein	Downhill uptake	$H^+$ :sugar stoichiometry	Uphill transport (accumulation)	$H^+$ leak	$H^+$ leak (+ sugar)
Wild type <sup>a</sup>	+	0.68–0.98	+	–	–
A177V/T <sup>b,c,d</sup>	+	0.57–0.74 <sup>LAC</sup> 0.84–0.89 <sup>TMG</sup>	+/-	+	↓
A177V/K319N <sup>d</sup>	+/-	0.30	–	+/-	↑
A177V/H322N <sup>e</sup>	+/-	0.84	–	ND	ND
Y236F/Y236H/Y236N/Y236S <sup>b,c</sup>	+/-	0.7	–	+	ND
R302S/R302H/R302L <sup>f</sup>	+/-	>0	+/-	–	↑
H322R <sup>g</sup>	+/-	ND	–	ND	ND
H322N <sup>h</sup>	+/-	0.82	+/-	ND	ND
H322F/Y <sup>i,j</sup>	+/-	>0	–	ND	ND

<sup>a</sup> Various references cited in this paper.

<sup>b</sup> Brooker *et al.*, 1985.

<sup>c</sup> King and Wilson, 1990b.

<sup>d</sup> Brooker, 1991.

<sup>e</sup> Brooker, 1990.

<sup>f</sup> Matzke *et al.*, 1992.

<sup>g</sup> Püttner *et al.*, 1989.

<sup>h</sup> Franco and Brooker, 1991.

<sup>i</sup> King and Wilson, 1989.

<sup>j</sup> King and Wilson, 1990a.

TABLE II  
The kinetic behavior of mutant enzymes with an ES leak and an EH leak

Properties of uncoupled mutants	
ES leak	EH leak
Accumulation levels decrease sigmoidally with increasing pH.	Accumulation levels increase sigmoidally with increasing pH.
H <sup>+</sup> : substrate stoichiometries decrease sigmoidally from 1 to 0 with increasing pH.	H <sup>+</sup> : substrate stoichiometries increase sigmoidally from <1 to >1 with increasing pH.
Coupling from initial rates is higher than from accumulation.	Coupling from initial rates is higher than from accumulation.
Coupling decreases with increasing substrate concentration.	Accumulation increases and initial rate ratios decrease with increasing substrate concentration.
The membrane potential is a better coupling force than the pH gradient.	The pH gradient is a better coupling force than the membrane potential.
Efflux inhibited by the membrane potential under conditions of no coupling (high pH).	Efflux not affected by the membrane potential under conditions of no coupling (low pH).

of transported cation and/or substrate.

The aim of the present study is to describe the steady state kinetic characteristics of the ES leak and EH leak type of mutants by simulating those experiments that are particularly discriminative. The major conclusions are as follows: (i) the two types of mutants can be discriminated easily by various criteria (summarized in Table II); (ii) in partially coupled systems, the degrees of coupling inferred from initial rates and accumulation are not the same; and (iii) the coupling characteristics are largely independent of the rate constants in the kinetic scheme.

Numerical analyses as used in this study require the assignment of numerical values to the rate constants pertinent to the kinetic scheme. The basic set of rate constants we have used represents a rather simple enzyme that is symmetrical with respect to the two sides of the membrane and in which the binding equilibria are rapid relative to the translocation equilibria. This choice improves the comprehensibility of the results. However, this set may not always be valid, *e.g.* functional asymmetry of secondary transporters has frequently been observed, and the binding equilibria are not necessarily fast relative to the translocation equilibria (Viitanen *et al.*, 1983; Page, 1987; Loo *et al.*, 1993). For this reason we have tested various additional schemes in which non-rapid binding equilibria, asymmetry, and cooperativity between the binding sites were introduced. The outcome of these analyses is that the coupling characteristics of the mutants described in this study do not differ much between the various schemes even though other kinetic parameters may be very different. Thus, the phenomena in the presented plots represent trends that are largely independent of the assumptions made in the original model. Importantly, the numbers should not be compared literally with any experimental data. Also, the analysis given in this study is one of extreme cases; the mutant carriers are characterized by one mobile and one immobile binary complex. Real mutations may affect the mobility of the two binary complexes differently, *i.e.* the *E*·S complex becomes more mobile than the *E*·H complex or the other way around. The observed phenotype will be according to the binary complex with the highest mobility, but the experimental behavior may differ in details from the analysis given here.

The lactose transport protein of *E. coli* is the most extensively studied bacterial transport system (for reviews see Kaback (1990); Poolman and Konings (1993)), and reports on LacY mutant characteristics provide ample evidence for the existence of ES leak and EH leak types of mutants (Table I). Various mutants of LacY have been isolated that are defective in uphill transport of galactosides but have a more or less normal H<sup>+</sup>:galactoside stoichiometry. This apparent discrepancy in the results is also observed in the mutants with the ES and the EH leak. It follows that  $n_{\text{grad}} \leq n_{\text{kin}}$  (Equations 1 and 2). In the case of the ES leak this is caused by the presence of the substrate inside the cell under conditions of accumulation. A

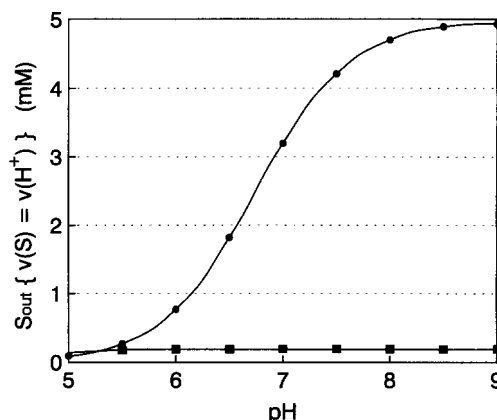


FIG. 6. Apparent complete coupling by the EH leak mutant from initial rate measurements. The substrate concentration at which the initial rates of uptake of proton and substrate are equal is plotted as a function of pH. The driving force consisted of a pH gradient of  $-60$  mV. The indicated pH is the external one. Substrate concentrations above and under the line result in proton:substrate stoichiometries that are lower and higher than 1, respectively. ●, rapid binding equilibrium; ■, non-rapid binding equilibrium.

significant internal substrate concentration introduces a futile cycle for the substrate via cycle Ib. Substrate that enters the cell via the ternary complex leaves the cell again via the ES leak while the proton stays inside. In the case of the EH leak the proton flux proceeds via the EH leak (cycle IIa) in the absence of substrate. Addition of the substrate induces a flux via the ternary complex, thereby decreasing the flux through the proton leak (see Scheme IC). At a particular substrate concentration the flux through the EH leak changes its direction from out-to-in to in-to-out. This is the point where the net substrate flux starts exceeding the net proton flux. Both substrate and proton enter the cell solely via the ternary complex, but part of the protons leave the cell again via the leak. The concentration needed to invert the flux through the EH leak depends strongly on the pH under the rapid binding equilibrium assumption (Fig. 2C, inset). Nevertheless, at each pH value a substrate concentration exists at which the coupling stoichiometry from initial rate measurements equals 1 (Fig. 6). Thus, a mutant with an EH leak may demonstrate an apparent full coupling between the proton and the substrate flux but, nevertheless, be unable to accumulate the substrate. The double mutant A177V/H322N of LacY is a clear example of this phenotype (Table I).

A wild-type proton symporter functioning at full activity will not significantly decrease the steady state proton motive force. The primary proton pumps can easily compensate for the substrate-coupled influx of protons via the carrier. This may be different when cells overproduce a transporter. Then, the increased "load" on the pmf may result in a decreased steady

state value of the pmf as is observed after addition of lactose to *E. coli* cells overexpressing the LacY protein (Brooker, 1991; King and Wilson, 1990b). On the other hand, overexpression of some LacY mutants (A177V/A177T, A177V/K319N, Y236F/Y236H/Y236N/Y236S, see Table I) results in a lowering of the pmf even in the absence of substrate. In the LacY-A177V mutant, this defect is reduced in the presence of the galactoside TDG, which restores the pmf to near normal values (King and Wilson, 1990b). The properties of this mutant are consistent with an EH leak (Fig. 4). The presence of substrate at both sides of the membrane reduces the flux through cycle IIa by pulling the enzyme in the enzyme-substrate complex. The double mutant A177V/K319N also exhibits a proton leak, which is reflected in a lowered pmf and an increased  $H^+$  leakage, but, in contrast to the single A177V mutant, this leak is enhanced in the presence of the non-metabolizable substrate TDG (Brooker, 1991). Expression of mutant LacY proteins in which Arg-302 is substituted for Ser, His, or Leu also causes a sugar-dependent  $H^+$  leak (and lowering of  $\Delta pH$ ) (Matzke *et al.*, 1992). The behavior of all these mutants mimics that of transport proteins with an ES leak pathway (Fig. 4). The enzyme-substrate complex functions as a facilitator for proton transport (cycle Ib), which is driven by the pmf. The presence of substrate at both sides of the membrane pulls the enzyme in the substrate-associated state. Saturation of the carrier with substrate results in the highest proton leak activity.

It is tempting to classify the various mutations of Table I as ES leak type or EH leak type. However, in general, the exper-

imental data is too incomplete to assign the mutants unambiguously to a particular leak type. The present analysis offers relatively simple means for further experimentation which should give a more solid basis for the classification. The data in Table I should be regarded as evidence for the validity of the two mechanisms of uncoupling analyzed in this paper.

**Acknowledgment**—We thank Prof. Dr. W. N. Konings for critical reading of the manuscript and many helpful suggestions.

#### REFERENCES

- Brooker, R. J. (1990) *J. Biol. Chem.* **265**, 4155–4160
- Brooker, R. J. (1991) *J. Biol. Chem.* **266**, 4131–4138
- Brooker, R. J., Fiebig, K., and Wilson, T. H. (1985) *J. Biol. Chem.* **260**, 16181–16186
- Franco, P. J., and Brooker, R. J. (1991) *J. Biol. Chem.* **266**, 6693–6699
- Garcia, M. L., Viitanen, P., Foster, D. L., and Kaback, H. R. (1983) *Biochem.* **22**, 2524–2531
- Kaback, H. R. (1990) *The Bacteria* Vol. XII, pp. 151–202, Academic Press, Inc., New York
- King, S. C., and Wilson, T. H. (1989) *J. Biol. Chem.* **264**, 7390–7394
- King, S. C., and Wilson, T. H. (1990a) *J. Biol. Chem.* **265**, 3153–3160
- King, S. C., and Wilson, T. H. (1990b) *J. Biol. Chem.* **265**, 9645–9651
- Krupka, R. M. (1993) *Biochim. Biophys. Acta* **1183**, 105–113
- Lolkema, J. S. (1993) *J. Biol. Chem.* **268**, 17850–17860
- Loo, D. F., Hazama, A., Supplisson, S., Turk, E., and Wright, E. M. (1993) *Proc. Natl. Acad. Sci. U. S. A.* **90**, 5767–5771
- Matzke, E. A., Stephenson, L. J., and Brooker, R. J. (1992) *J. Biol. Chem.* **267**, 19095–19100
- Page, M. G. P. (1987) *Biochim. Biophys. Acta* **897**, 112–126
- Poolman, B., and Konings, W. N. (1993) *Biochim. Biophys. Acta* **1183**, 5–39
- Püttner, I. B., Sarkar, H. K., Padan, E., Lolkema, J. S., and Kaback, H. R. (1989) *Biochemistry* **28**, 2525–2533
- Viitanen, P., Garcia, M. L., Foster, D. L., and Kaback, H. R. (1993) *Biochemistry* **22**, 2524–2531